The effect of increased water vapor from the Hunga Tonga-Hunga Ha'apai eruption on the Antarctic ozone hole

Ingo Wohltmann[1], Michelle L. Santee[2], Gloria L Manney[3], and Luis Millan[4]

[1]Alfred Wegener Institute for Polar and Marine Research
[2]Jet Propulsion Laboratory
[3]Northwest Research Associates
[4]Jet propulsion laboratory

November 8, 2023

Abstract

The eruption of the Hunga Tonga-Hunga Ha'apai volcano on 15 January 2022 was one of the most explosive eruptions of the last decades. The unprecedented amount of water vapor injected into the stratosphere increased the stratospheric water vapor burden by about 10%. Using model runs from the ATLAS chemistry and transport model and Microwave Limb Sounder (MLS) satellite observations, we show that while 20-40% more water vapor than usual was entrained into the Antarctic polar vortex as it formed (e.g., typical values of 4.6 ppm at 21.5 km increased to 6.7 ppm), the direct effect of the increased water vapor on Antarctic ozone depletion was minor. This is caused by the very low temperatures in the vortex, which limit water vapor to the saturation pressure and tend to reset any anomalies in water vapor by dehydration before they can have an effect on ozone loss.

The effect of increased water vapor from the Hunga Tonga-Hunga Ha'apai eruption on the Antarctic ozone hole

Ingo Wohltmann[1]

Michelle L. Santee[2]

Gloria L. Manney[3,4]

Luis F. Millán[2]

[1]Alfred Wegener Institute, Helmholtz Centre for Polar and Marine Research, Potsdam, Germany
[2]Jet Propulsion Laboratory, California Institute of Technology, Pasadena, CA, USA
[3]NorthWest Research Associates, Socorro, NM, USA
[4]New Mexico Institute of Mining and Technology, Socorro, NM, USA

Key Points:

- The Hunga Tonga-Hunga Ha'apai eruption increased water vapor in the emerging Antarctic vortex in 2023 by 20–40 % compared to earlier years.
- The direct effect of the increased water vapor from the Hunga Tonga-Hunga Ha'apai eruption on Antarctic ozone depletion was minor.
- The small effect is attributable to low vortex temperatures, which tend to reset anomalies in water vapor before they can affect ozone loss.

Corresponding author: Ingo Wohltmann, ingo.wohltmann@awi.de

Abstract

The eruption of the Hunga Tonga-Hunga Ha'apai volcano on 15 January 2022 was one of the most explosive eruptions of the last decades. The unprecedented amount of water vapor injected into the stratosphere increased the stratospheric water vapor burden by about 10 %. Using model runs from the ATLAS chemistry and transport model and Microwave Limb Sounder (MLS) satellite observations, we show that while 20–40% more water vapor than usual was entrained into the Antarctic polar vortex as it formed (e.g., typical values of 4.6 ppm at 21.5 km increased to 6.7 ppm), the direct effect of the increased water vapor on Antarctic ozone depletion was minor. This is caused by the very low temperatures in the vortex, which limit water vapor to the saturation pressure and tend to reset any anomalies in water vapor by dehydration before they can have an effect on ozone loss.

Plain Language Summary

The eruption of the Hunga Tonga-Hunga Ha'apai volcano on 15 January 2022 was one of the most explosive eruptions of the last decades. An unprecedented amount of water vapor was injected into the stratosphere, increasing the total stratospheric water vapor mass by about 10 %. Using model runs and satellite observations, we show that while the dissipation of the plume increased water vapor in the Antarctic in 2023 by 20–40 % at the beginning of the ozone hole season compared to earlier years, the effect of the increased water vapor on the Antarctic ozone hole was minor. This is caused by the very low temperatures in the vortex, which limit water vapor due to condensation and tend to reset any anomalies in water vapor before they can have an effect on ozone loss and sedimentation of condensed particles.

1 Introduction

The eruption of the Hunga Tonga-Hunga Ha'apai volcano on 15 January 2022 was one of the most violent eruptions of the last decades. It reached a volcanic explosivity index (VEI) of 5, and the plume reached an altitude of more than 50 km (e.g. Carr et al., 2022; Millán et al., 2022; Proud et al., 2022; Schoeberl et al., 2022). An unprecedented amount of water vapor was injected into the stratosphere, increasing the stratospheric water vapor burden by about 10% or 150 Tg (Millán et al., 2022; Schoeberl et al., 2022; Vömel et al., 2022). While the increased water vapor was not able to penetrate into the 2022 Antarctic vortex (Manney et al., 2023), the dissipating plume increased water vapor observed by MLS in the developing Antarctic vortex in 2023 by about 20 % to 40 % compared to earlier years (in the pressure range of 56.2–17.7 hPa or approximate altitude range 20–28 km). Figure 1 (a) shows vortex-averaged profiles of MLS measurements of water vapor (version 5, (Livesey et al., 2022)) in the developing Antarctic vortex for all years of the MLS record (2005–2023) on 20 May. Here and in the following, the vortex is defined as the volume inside the −36 PVU contour of modified potential vorticity (which scales potential vorticity to have a similar range of values throughout the stratosphere) calculated from a reference level of $\theta_0 = 475\,\mathrm{K}$ (Lait, 1994). Typical profiles at the end of May in the years before 2023 are very similar. In comparison, the profile of 2023 shows increased values throughout a large vertical range. For example, values at 21.5 km increased from an average 4.6 ppm in earlier years to 6.7 ppm in 2023.

It was speculated that the increased water vapor from the eruption could lead to increased ozone depletion in the Antarctic ozone hole in 2023 (e.g. Millán et al., 2022; Manney et al., 2023). Water vapor can influence polar ozone depletion mainly by its effect on polar stratospheric clouds (PSCs), e.g. by changes in formation temperature thresholds, particle size distribution, or dehydration and denitrification. However, MLS measurements in 2023 show that ozone values are not exceptional and are well within the range of earlier years. This can be seen in Figure 1 (h), which shows vortex-averaged profiles of MLS measurements of ozone on 1 October after the end of the most severe ozone loss period.

However, it is not possible to attribute interannual changes in ozone to changes in water vapor based on measurements alone. Interannual differences in temperature, transport, or the amount of ozone-depleting species can have a significant effect on the interannual variability.

2 Model setup

We perform runs of the ATLAS chemistry and transport model (Wohltmann & Rex, 2009; Wohltmann et al., 2010) to disentangle the effects of water vapor and other factors such as temperature. A reference run is initialized with the MLS data from 1 May 2023. A sensitivity run uses exactly the same setup, with the exception of the initialization of MLS water vapor, which is taken from the preceding year on 1 May 2022 (i.e., without the effect of Hunga Tonga on water vapor).

The model setup is almost the same as that in Wohltmann et al. (2021), and we refer the reader to that paper for more details. Model runs are driven by meteorological data from the European Center of Medium-Range Weather Forecasts (ECMWF) ERA5 reanalysis (provided on a $1.125^{\circ} \times 1.125^{\circ}$ horizontal grid, 3 h temporal resolution, and 137 model levels) (Hersbach et al., 2017, 2020). The ATLAS model resolution is 150 km. The model was run from 1 April 2023 to 1 October 2023. Chemical species are initialized after a spin-up period of 1 month on 1 May. O_3, H_2O, HCl, N_2O, HNO_3, and CO are initialized from all MLS measurements on 1 May for the reference run. The other chemical species are initialized from climatologies as described in Wohltmann et al. (2021).

While we refer to the model description papers for most details of the PSC parameterization, the parameterization of dehydration is important for our study. Dehydration is modelled in a deliberately simple fashion in ATLAS, which is justified by the good agreement with observations. Above a given supersaturation, all water vapor is removed from the model instantaneously. For this study, we use a value for supersaturation of 0.7. The value was empirically adjusted to fit the water vapor measurements in earlier studies.

3 Results

Figure 2 (a) shows the time evolution of vortex-averaged water vapor in the reference run, the sensitivity run, and in the MLS data at 475 K potential temperature. The reference run and MLS show excellent agreement over the complete time period. Water vapor starts with values of about 6–7 ppm in May, but quickly decreases to values of about 3–4 ppm between mid-May and the start of July. This decrease is caused by dehydration, which limits water vapor to the saturation pressure through condensation and sedimentation in the very cold polar vortex. The decrease is also visible in the MLS profiles in Figures 1 (c, e, g), except at the highest altitudes where water vapor does not exceed the saturation limit. Figures 1 (c, e, g) also show that water vapor is well within the range of previous years by the beginning of July.

Figure 2 (a) shows that the sensitivity run starts at values below 5 ppm that do not agree well with the measurements (as expected). However, the sensitivity run quickly converges to the reference run by early July. This is because in both cases the temperatures are sufficiently low that water vapor abundances are mostly above the saturation limit. Once the saturation limit is reached, water vapor in both runs is equalized.

Figure 2 (b) shows the corresponding time evolution of vortex-averaged ozone at 475 K. The difference between the reference run and the sensitivity run is very small throughout the whole time period. This is because heterogeneous ozone loss is only significant

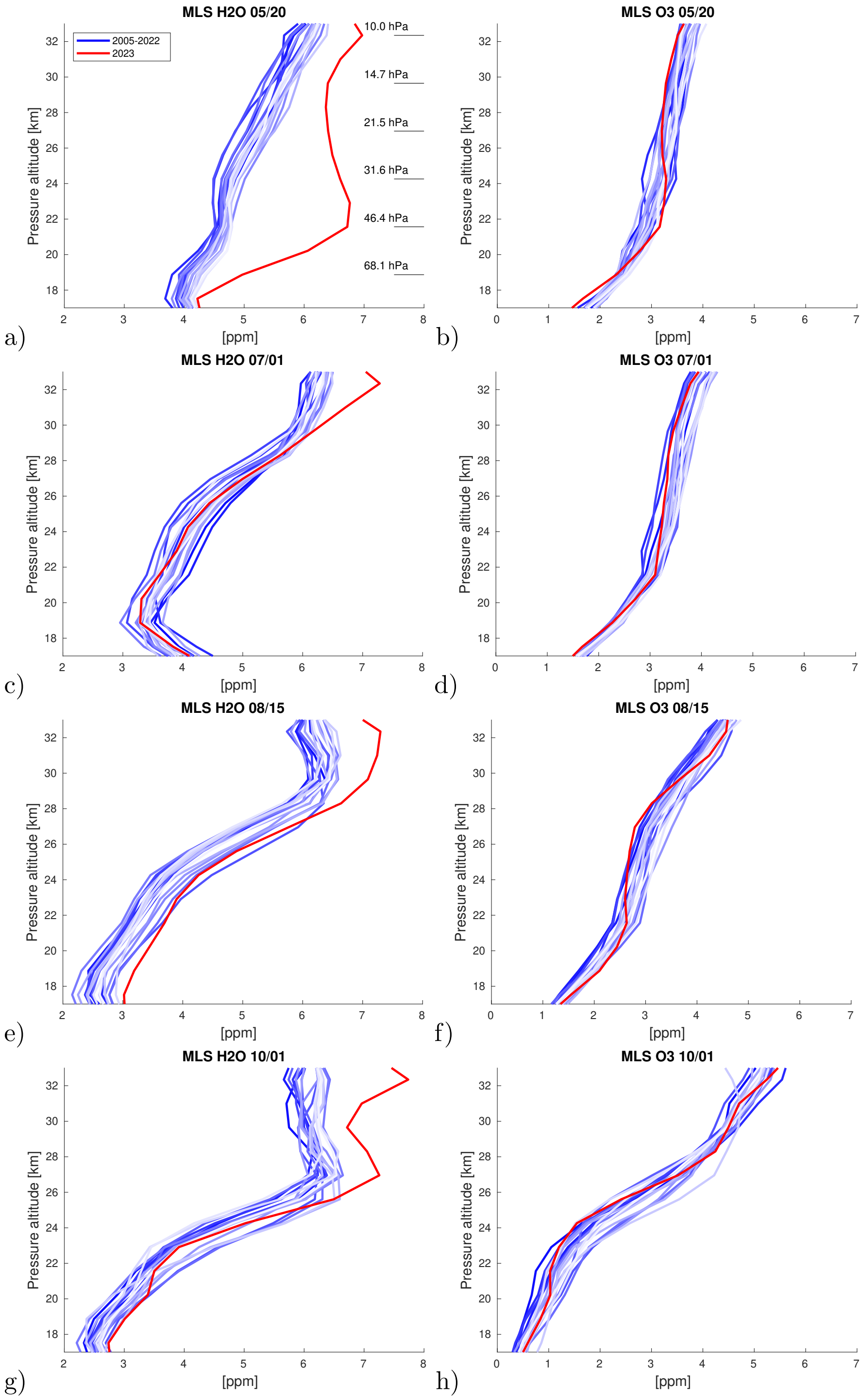

Figure 1. Left: Vortex-averaged water vapor profiles observed by MLS on 20 May (a), 1 July (c), 15 August (e) and 1 October (g) for all years of the MLS data record. 2005–2022 in shades of blue, 2023 is highlighted in red. Right: Same for ozone (b, d, f, h). Profiles are averaged over all MLS measurements of the given day inside the -36 PVU contour of modified potential vorticity. Every other MLS pressure level is indicated in panel (a).

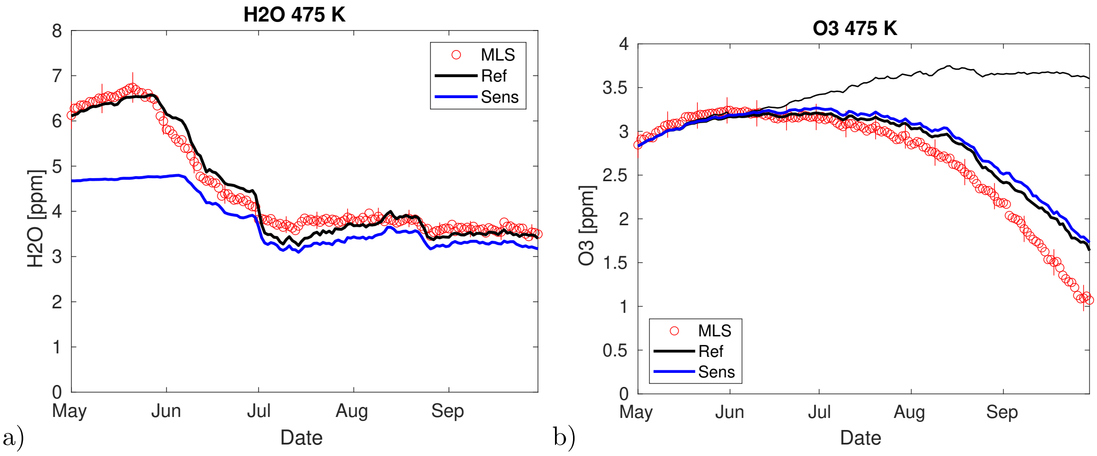

Figure 2. Left (a): Vortex-averaged water vapor at 475 K potential temperature observed by MLS in 2023 (red dots) and modelled by ATLAS (blue and black lines). The black line shows the reference run initialized with MLS measurements from 2023, while the blue line shows the sensitivity run initialized with MLS water vapor data from 2022 (i.e., without the effect of Hunga Tonga on water vapor). Right (b): Same for ozone. The thin black line shows a passive ozone tracer initialized on 1 June. The difference between the thin black line and the other lines quantifies the amount of ozone loss.

within the sunlit portion of the vortex from July through September. The thin black line shows a passive ozone tracer initialized on 1 June. The difference between the passive ozone tracer and the other lines quantifies the amount of ozone loss. There is only a short time period before July (cf. Figure 2 (a)) when differences in water vapor between the runs can have a direct effect on differences in ozone loss.

The difference between the modelled ozone and the passive ozone tracer underestimates ozone loss by about 0.7 ppm (30 %) compared to the difference between the passive ozone tracer and MLS ozone. Since ATLAS runs for other Antarctic winters agree better with MLS (e.g., Wohltmann et al., 2021), this discrepancy might hint that other effects from the Hunga Tonga eruption are at work. However, as outlined before, it cannot be the direct effect of water vapor.

The results at other potential temperature levels lead to similar conclusions, and the effect of the increased water vapor remains small throughout the ozone column. Figure 3 shows the chemical ozone loss modelled by ATLAS for the partial column from the lower model boundary at 157 hPa to 28.6 hPa. Ozone loss was determined by subtracting the passive ozone tracer initialized on 1 June from the modelled ozone values. Since the value of the passive ozone tracer is not known for air masses that entered through the upper model boundary after 1 June and descended in the vortex, the column is restricted to 28.6 hPa. The figure shows that the effect of the increased water vapor on the column loss in the model is small.

4 Discussion and Summary

There are several ways in which water vapor might change ozone loss in addition to dehydration:

- The threshold temperatures for the formation of all PSC types (supercooled ternary solution (STS), nitric acid trihydrate (NAT) and ice) are increased by the increased

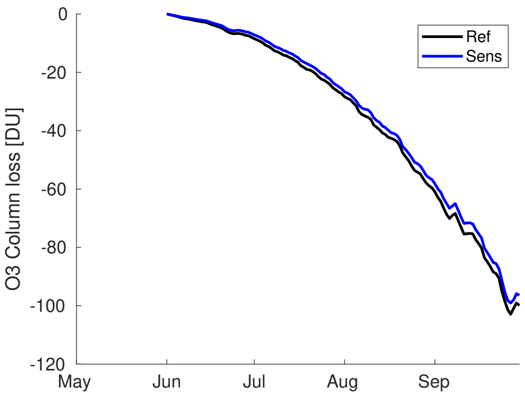

Figure 3. Vortex-averaged chemical loss of ozone modelled by ATLAS for the partial column from the lower model boundary at 157 hPa to 28.6 hPa. The black line shows the reference run initialized with MLS measurements from 2023, while the blue line shows the sensitivity run initialized with MLS water vapor data from 2022 (i.e., without the effect of Hunga Tonga on water vapor).

water vapor. For example, a change in water vapor from 5 ppm to 6 ppm increases the threshold temperature for ice by 1.1 K at 50 hPa (Marti & Mauersberger, 1993), and for NAT by 0.8 K (for a HNO_3 mixing ratio of 10 ppb) (D. Hanson & Mauersberger, 1988). STS has no defined threshold temperature for formation but shows a gradual increase of reaction rates and droplet volume with lower temperatures. However, an increase in water vapor from 5 ppm to 6 ppm has to a good approximation the same effect on the STS reactivity (time needed for the HCl+$ClONO_2$ reaction to completely deplete one of the reaction partners) as a temperature change of 1 K (D. R. Hanson & Ravishankara, 1994; Carslaw et al., 1995) (for 2 ppb HCl, 1 ppb $ClONO_2$, 0.15 ppb H_2SO_4, number density of droplets 10 cm^{-3}).
While these changes increase the volume inside the vortex where the formation of PSCs is possible, this can only have an effect before dehydration sets in. The effects of changes in threshold temperatures and STS reactivity are included in ATLAS. Figure 2 (b) shows that they have no large effect on ozone depletion.

- Changes in water vapor have an effect on the particle size distribution of all cloud types. There is more water vapor available above the saturation limit, and one might expect larger particle sizes and larger surface area densities. However, particle formation and growth is a complex process, and this might not be straightforward.
As in many chemistry and transport models, PSCs are treated in a somewhat simplified manner in ATLAS (Tritscher et al., 2021). For NAT and ice clouds, a constant number density is assumed, and a uniform particle size is then calculated from the HNO_3 and H_2O available above the saturation pressure. That is, the uniform particle size will simply increase in our model. For STS, a constant number density and a log-normal distribution is assumed that is scaled with the total liquid volume.
Figure 2 (b) shows that changes in size distribution have only a small effect on ozone depletion in ATLAS. However, particle growth and formation might be more complex in reality and the effect on ozone depletion may be larger. Changes in size distribution may also have an effect after dehydration sets in (i.e., differences in the size distribution of NAT, ice and STS PSCs caused by increased water vapor in May and June might be persistent or lead to changes in the size distribution in later months).

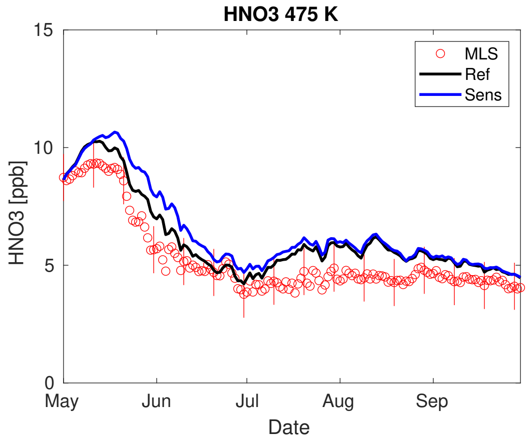

Figure 4. Vortex-averaged HNO_3 (gas phase) at 475 K potential temperature observed by MLS in 2023 (red dots) and modelled by ATLAS (blue and black lines). The black line shows the reference run initialized with MLS measurements from 2023, while the blue line shows the sensitivity run initialized with MLS water vapor data from 2022 (i.e., without the effect of Hunga Tonga on water vapor).

- Since larger particles have a greater fall velocity, dehydration might also be faster in 2023. However, this is not considered in the simple ATLAS dehydration parameterization. The good agreement between ATLAS and MLS suggests that dehydration might be a fast enough process so that the speed of the process does not matter for the amount of ozone depletion.
- Denitrification might also be affected by differences in the formation of the NAT particles. Denitrification is treated in a more sophisticated manner than dehydration in ATLAS and incorporates the nucleation, growth, sedimentation, and evaporation of individual particles with the DLAPSE model (Davies et al., 2005). Figure 4 shows that the changes in gas-phase HNO_3 (which are mainly caused by denitrification) are small between the reference run and the sensitivity run.

In summary, we have shown that while the Hunga Tonga-Hunga Ha'apai eruption increased water vapor in the emerging Southern Hemisphere stratospheric polar vortex by 20–40 % in 2023, ozone values at the end of September in the Antarctic ozone hole were in no way exceptional and were well within in the range of earlier years. ATLAS model runs indicate that the direct effect of the increased water vapor on Antarctic ozone depletion was minor. The reason for this are the very low temperatures in the vortex, which limit water vapor to the saturation pressure and tend to reset any anomalies in water vapor through dehydration before they can have an effect on ozone loss. However, the ATLAS runs underestimate observed ozone loss in 2023 by about 30 % (in contrast to good agreement with observations in similar studies for other winters). Further studies would be needed to understand the causes of this discrepancy and whether it may be related to other effects from the Hunga Tonga-Huga Ha'apai eruption in addition to the increased water vapor and dehydration.

Open Research Section

ATLAS source code is available from the repository at https://gitlab.awi.de/iwohltmann/atlas-julia. MLS data are available at https://disc.gsfc.nasa.gov/datasets?page=1&keywords=AURA%20MLS. ECMWF ERA5 data are available at Hersbach et al. (2017), doi:10.24381/cds.143582cf.

Acknowledgments

ECMWF ERA5 and ERA5T data (Hersbach et al., 2017) was downloaded from the Copernicus Climate Change Service (C3S) (2023). The results contain modified Copernicus Climate Change Service information 2023. Neither the European Commission nor ECMWF is responsible for any use that may be made of the Copernicus information or data it contains.

Work at the Jet Propulsion Laboratory, California Institute of Technology, was carried out under a contract with the National Aeronautics and Space Administration (80NM0018D0004). G. L. Manney was supported by the Jet Propulsion Laboratory (JPL) Microwave Limb Sounder team under JPL subcontract #1521127 to NWRA.

We thank Peter von der Gathen for helpful comments and discussion.

References

Carr, J. L., Horváth, Á., Wu, D. L., & Friberg, M. D. (2022). Stereo plume height and motion retrievals for the record-setting Hunga Tonga-Hunga Ha'apai eruption of 15 January 2022. *Geophys. Res. Lett.*, *49*. doi: 10.1029/2022GL098131

Carslaw, K. S., Clegg, S. L., & Brimblecombe, P. (1995). A thermodynamic model of the system HCl-HNO3-H2SO4-H2O, including solubilities of HBr, from < 200 to 328 k. *J. Phys. Chem.*, *99*(29), 11557-11574. doi: 10.1021/j100029a039

Davies, S., Mann, G. W., Carslaw, K. S., Chipperfield, M. P., Kettleborough, J. A., Santee, M. L., ... Sugita, T. (2005). 3-D microphysical model studies of Arctic denitrification: comparison with observations. *Atmos. Chem. Phys.*, *5*, 3093-3109. doi: 10.5194/acp-5-3093-2005

Hanson, D., & Mauersberger, K. (1988). Laboratory studies of the nitric acid trihydrate: Implications for the south polar stratosphere. *Geophys. Res. Lett.*, *15*(8), 855-858. doi: 10.1029/GL015i008p00855

Hanson, D. R., & Ravishankara, A. R. (1994). Reactive uptake of ClONO2 onto sulfuric acid due to reaction with HCl and H2O. *J. Phys. Chem.*, *98*(22), 5728-5735. doi: 10.1021/j100073a026

Hersbach, H., Bell, B., Berrisford, P., S., Hirahara, Horányi, A., Muñoz-Sabater, J., ... Thépaut, J.-N. (2017). Complete ERA5 from 1940: Fifth generation of ECMWF atmospheric reanalyses of the global climate. Copernicus Climate Change Service (C3S) Data Store (CDS). (Accessed on DD-MMM-YYYY). doi: 10.24381/cds.143582cf

Hersbach, H., Bell, B., Berrisford, P., Hirahara, S., Horányi, A., Muñoz-Sabater, J., ... Thépaut, J.-N. (2020). The ERA5 global reanalysis. *Quarterly Journal of the Royal Meteorological Society*, *146*, 1999-2049. doi: 10.1002/qj.3803

Lait, L. R. (1994). An alternative form for potential vorticity. *J. Atmos. Sci.*, *51*(12), 1754-1759.

Livesey, N. J., Read, W. G., Wagner, P. A., Froidevaux, L., Santee, M. L., Schwartz, M. J., ... Lay, R. R. (2022). *Earth Observing System (EOS) Aura Microwave Limb Sounder (MLS) version 5.0x level 2 and 3 data quality and description document.* JPL D-105336 Rev. B.

Manney, G. L., Santee, M. L., Lambert, A., Millán, L. F., Minschwaner, K., Werner, F., ... Wang, T. (2023). Siege in the southern stratosphere: Hunga Tonga-Hunga Ha'apai water vapor excluded from the 2022 Antarctic polar vortex. *Geophys. Res. Lett.*, *50*. doi: 10.1029/2023GL103855

Marti, J., & Mauersberger, K. (1993). A survey and new measurements of ice vapor pressure at temperatures between 170 and 250 k. *Geophys. Res. Lett.*, *20*, 363-366. doi: 10.1029/93GL00105

Millán, L., Santee, M. L., Lambert, A., Livesey, N. J., Werner, F., Schwartz, M. J.,

… Froidevaux, L. (2022). The Hunga Tonga-Hunga Ha'apai hydration of the stratosphere. *Geophys. Res. Lett.*, *49*. doi: 10.1029/2022GL099381

Proud, S. R., Prata, A. T., & Schmauß, S. (2022). The January 2022 eruption of Hunga Tonga-Hunga Ha'apai volcano reached the mesosphere. *Science*, *378*(6619), 554-557. doi: 10.1126/science.abo407

Schoeberl, M. R., Wang, Y., Ueyama, R., Taha, G., Jensen, E., & Yu, W. (2022). Analysis and impact of the Hunga Tonga-Hunga Ha'apai stratospheric water vapor plume. *Geophys. Res. Lett.*. doi: 10.1029/2022GL100248

Tritscher, I., Pitts, M. C., Poole, L. R., Alexander, S. P., Cairo, F., Chipperfield, M. P., … Peter, T. (2021). Polar stratospheric clouds: Satellite observations, processes, and role in ozone depletion. *Reviews of Geophysics*, *59*(2). doi: 10.1029/2020RG000702

Vömel, H., Evan, S., & Tully, M. (2022). Water vapor injection into the stratosphere by Hunga Tonga-Hunga Ha'apai. *Science*, *377*, 1444-1447. doi: 10.1126/science.abq2299

Wohltmann, I., Lehmann, R., & Rex, M. (2010). The Lagrangian chemistry and transport model ATLAS: simulation and validation of stratospheric chemistry and ozone loss in the winter 1999/2000. *Geosci. Model Dev.*, *3*, 585-601.

Wohltmann, I., & Rex, M. (2009). The Lagrangian chemistry and transport model ATLAS: validation of advective transport and mixing. *Geosci. Model Dev.*, *2*, 153-173.

Wohltmann, I., von der Gathen, P., Lehmann, R., Deckelmann, H., Manney, G. L., Davies, J., … Rex, M. (2021). Chemical evolution of the exceptional Arctic stratospheric winter 2019/2020 compared to previous Arctic and Antarctic winters. *J. Geophys. Res. Atmos.*, *126*. doi: 10.1029/2020JD034356

The effect of increased water vapor from the Hunga Tonga-Hunga Ha'apai eruption on the Antarctic ozone hole

Ingo Wohltmann[1]

Michelle L. Santee[2]

Gloria L. Manney[3,4]

Luis F. Millán[2]

[1]Alfred Wegener Institute, Helmholtz Centre for Polar and Marine Research, Potsdam, Germany
[2]Jet Propulsion Laboratory, California Institute of Technology, Pasadena, CA, USA
[3]NorthWest Research Associates, Socorro, NM, USA
[4]New Mexico Institute of Mining and Technology, Socorro, NM, USA

Key Points:

- The Hunga Tonga-Hunga Ha'apai eruption increased water vapor in the emerging Antarctic vortex in 2023 by 20–40 % compared to earlier years.
- The direct effect of the increased water vapor from the Hunga Tonga-Hunga Ha'apai eruption on Antarctic ozone depletion was minor.
- The small effect is attributable to low vortex temperatures, which tend to reset anomalies in water vapor before they can affect ozone loss.

Corresponding author: Ingo Wohltmann, ingo.wohltmann@awi.de

Abstract

The eruption of the Hunga Tonga-Hunga Ha'apai volcano on 15 January 2022 was one of the most explosive eruptions of the last decades. The unprecedented amount of water vapor injected into the stratosphere increased the stratospheric water vapor burden by about 10 %. Using model runs from the ATLAS chemistry and transport model and Microwave Limb Sounder (MLS) satellite observations, we show that while 20–40% more water vapor than usual was entrained into the Antarctic polar vortex as it formed (e.g., typical values of 4.6 ppm at 21.5 km increased to 6.7 ppm), the direct effect of the increased water vapor on Antarctic ozone depletion was minor. This is caused by the very low temperatures in the vortex, which limit water vapor to the saturation pressure and tend to reset any anomalies in water vapor by dehydration before they can have an effect on ozone loss.

Plain Language Summary

The eruption of the Hunga Tonga-Hunga Ha'apai volcano on 15 January 2022 was one of the most explosive eruptions of the last decades. An unprecedented amount of water vapor was injected into the stratosphere, increasing the total stratospheric water vapor mass by about 10 %. Using model runs and satellite observations, we show that while the dissipation of the plume increased water vapor in the Antarctic in 2023 by 20–40 % at the beginning of the ozone hole season compared to earlier years, the effect of the increased water vapor on the Antarctic ozone hole was minor. This is caused by the very low temperatures in the vortex, which limit water vapor due to condensation and tend to reset any anomalies in water vapor before they can have an effect on ozone loss and sedimentation of condensed particles.

1 Introduction

The eruption of the Hunga Tonga-Hunga Ha'apai volcano on 15 January 2022 was one of the most violent eruptions of the last decades. It reached a volcanic explosivity index (VEI) of 5, and the plume reached an altitude of more than 50 km (e.g. Carr et al., 2022; Millán et al., 2022; Proud et al., 2022; Schoeberl et al., 2022). An unprecedented amount of water vapor was injected into the stratosphere, increasing the stratospheric water vapor burden by about 10% or 150 Tg (Millán et al., 2022; Schoeberl et al., 2022; Vömel et al., 2022). While the increased water vapor was not able to penetrate into the 2022 Antarctic vortex (Manney et al., 2023), the dissipating plume increased water vapor observed by MLS in the developing Antarctic vortex in 2023 by about 20 % to 40 % compared to earlier years (in the pressure range of 56.2–17.7 hPa or approximate altitude range 20–28 km). Figure 1 (a) shows vortex-averaged profiles of MLS measurements of water vapor (version 5, (Livesey et al., 2022)) in the developing Antarctic vortex for all years of the MLS record (2005–2023) on 20 May. Here and in the following, the vortex is defined as the volume inside the −36 PVU contour of modified potential vorticity (which scales potential vorticity to have a similar range of values throughout the stratosphere) calculated from a reference level of $\theta_0 = 475\,\mathrm{K}$ (Lait, 1994). Typical profiles at the end of May in the years before 2023 are very similar. In comparison, the profile of 2023 shows increased values throughout a large vertical range. For example, values at 21.5 km increased from an average 4.6 ppm in earlier years to 6.7 ppm in 2023.

It was speculated that the increased water vapor from the eruption could lead to increased ozone depletion in the Antarctic ozone hole in 2023 (e.g. Millán et al., 2022; Manney et al., 2023). Water vapor can influence polar ozone depletion mainly by its effect on polar stratospheric clouds (PSCs), e.g. by changes in formation temperature thresholds, particle size distribution, or dehydration and denitrification. However, MLS measurements in 2023 show that ozone values are not exceptional and are well within the range of earlier years. This can be seen in Figure 1 (h), which shows vortex-averaged profiles of MLS measurements of ozone on 1 October after the end of the most severe ozone loss period.

However, it is not possible to attribute interannual changes in ozone to changes in water vapor based on measurements alone. Interannual differences in temperature, transport, or the amount of ozone-depleting species can have a significant effect on the interannual variability.

2 Model setup

We perform runs of the ATLAS chemistry and transport model (Wohltmann & Rex, 2009; Wohltmann et al., 2010) to disentangle the effects of water vapor and other factors such as temperature. A reference run is initialized with the MLS data from 1 May 2023. A sensitivity run uses exactly the same setup, with the exception of the initialization of MLS water vapor, which is taken from the preceding year on 1 May 2022 (i.e., without the effect of Hunga Tonga on water vapor).

The model setup is almost the same as that in Wohltmann et al. (2021), and we refer the reader to that paper for more details. Model runs are driven by meteorological data from the European Center of Medium-Range Weather Forecasts (ECMWF) ERA5 reanalysis (provided on a 1.125° × 1.125° horizontal grid, 3 h temporal resolution, and 137 model levels) (Hersbach et al., 2017, 2020). The ATLAS model resolution is 150 km. The model was run from 1 April 2023 to 1 October 2023. Chemical species are initialized after a spin-up period of 1 month on 1 May. O_3, H_2O, HCl, N_2O, HNO_3, and CO are initialized from all MLS measurements on 1 May for the reference run. The other chemical species are initialized from climatologies as described in Wohltmann et al. (2021).

While we refer to the model description papers for most details of the PSC parameterization, the parameterization of dehydration is important for our study. Dehydration is modelled in a deliberately simple fashion in ATLAS, which is justified by the good agreement with observations. Above a given supersaturation, all water vapor is removed from the model instantaneously. For this study, we use a value for supersaturation of 0.7. The value was empirically adjusted to fit the water vapor measurements in earlier studies.

3 Results

Figure 2 (a) shows the time evolution of vortex-averaged water vapor in the reference run, the sensitivity run, and in the MLS data at 475 K potential temperature. The reference run and MLS show excellent agreement over the complete time period. Water vapor starts with values of about 6–7 ppm in May, but quickly decreases to values of about 3–4 ppm between mid-May and the start of July. This decrease is caused by dehydration, which limits water vapor to the saturation pressure through condensation and sedimentation in the very cold polar vortex. The decrease is also visible in the MLS profiles in Figures 1 (c, e, g), except at the highest altitudes where water vapor does not exceed the saturation limit. Figures 1 (c, e, g) also show that water vapor is well within the range of previous years by the beginning of July.

Figure 2 (a) shows that the sensitivity run starts at values below 5 ppm that do not agree well with the measurements (as expected). However, the sensitivity run quickly converges to the reference run by early July. This is because in both cases the temperatures are sufficiently low that water vapor abundances are mostly above the saturation limit. Once the saturation limit is reached, water vapor in both runs is equalized.

Figure 2 (b) shows the corresponding time evolution of vortex-averaged ozone at 475 K. The difference between the reference run and the sensitivity run is very small throughout the whole time period. This is because heterogeneous ozone loss is only significant

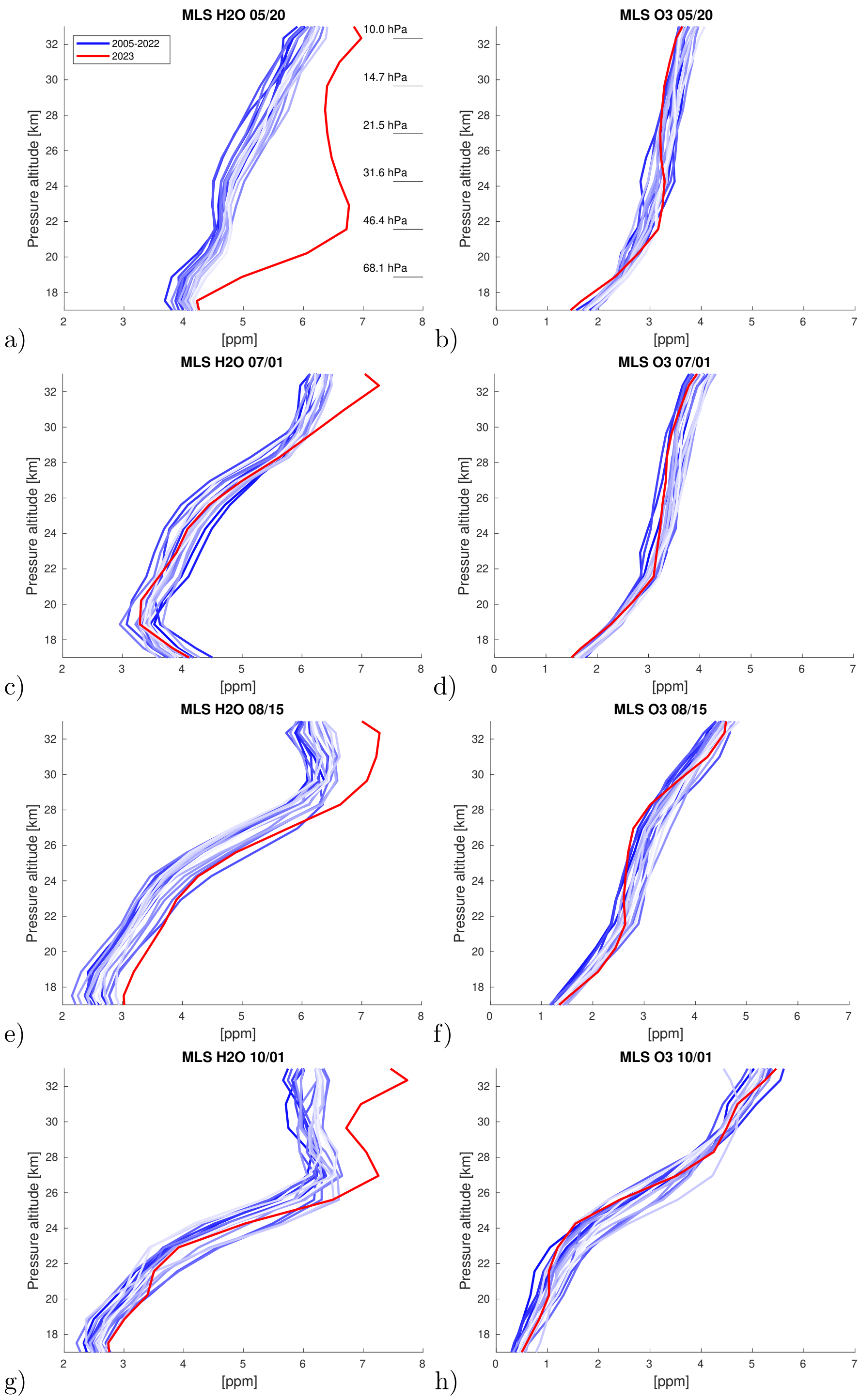

Figure 1. Left: Vortex-averaged water vapor profiles observed by MLS on 20 May (a), 1 July (c), 15 August (e) and 1 October (g) for all years of the MLS data record. 2005–2022 in shades of blue, 2023 is highlighted in red. Right: Same for ozone (b, d, f, h). Profiles are averaged over all MLS measurements of the given day inside the -36 PVU contour of modified potential vorticity. Every other MLS pressure level is indicated in panel (a).

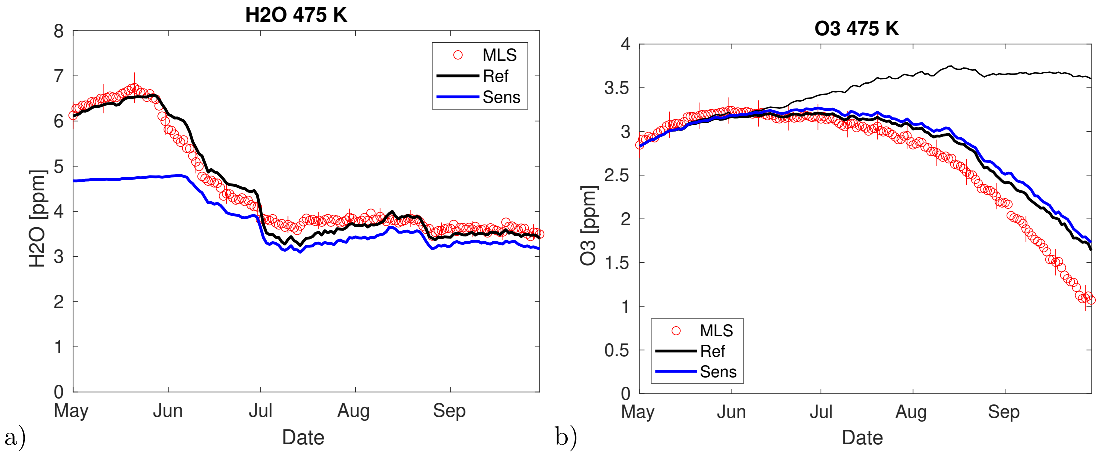

Figure 2. Left (a): Vortex-averaged water vapor at 475 K potential temperature observed by MLS in 2023 (red dots) and modelled by ATLAS (blue and black lines). The black line shows the reference run initialized with MLS measurements from 2023, while the blue line shows the sensitivity run initialized with MLS water vapor data from 2022 (i.e., without the effect of Hunga Tonga on water vapor). Right (b): Same for ozone. The thin black line shows a passive ozone tracer initialized on 1 June. The difference between the thin black line and the other lines quantifies the amount of ozone loss.

within the sunlit portion of the vortex from July through September. The thin black line shows a passive ozone tracer initialized on 1 June. The difference between the passive ozone tracer and the other lines quantifies the amount of ozone loss. There is only a short time period before July (cf. Figure 2 (a)) when differences in water vapor between the runs can have a direct effect on differences in ozone loss.

The difference between the modelled ozone and the passive ozone tracer underestimates ozone loss by about 0.7 ppm (30 %) compared to the difference between the passive ozone tracer and MLS ozone. Since ATLAS runs for other Antarctic winters agree better with MLS (e.g., Wohltmann et al., 2021), this discrepancy might hint that other effects from the Hunga Tonga eruption are at work. However, as outlined before, it cannot be the direct effect of water vapor.

The results at other potential temperature levels lead to similar conclusions, and the effect of the increased water vapor remains small throughout the ozone column. Figure 3 shows the chemical ozone loss modelled by ATLAS for the partial column from the lower model boundary at 157 hPa to 28.6 hPa. Ozone loss was determined by subtracting the passive ozone tracer initialized on 1 June from the modelled ozone values. Since the value of the passive ozone tracer is not known for air masses that entered through the upper model boundary after 1 June and descended in the vortex, the column is restricted to 28.6 hPa. The figure shows that the effect of the increased water vapor on the column loss in the model is small.

4 Discussion and Summary

There are several ways in which water vapor might change ozone loss in addition to dehydration:

- The threshold temperatures for the formation of all PSC types (supercooled ternary solution (STS), nitric acid trihydrate (NAT) and ice) are increased by the increased

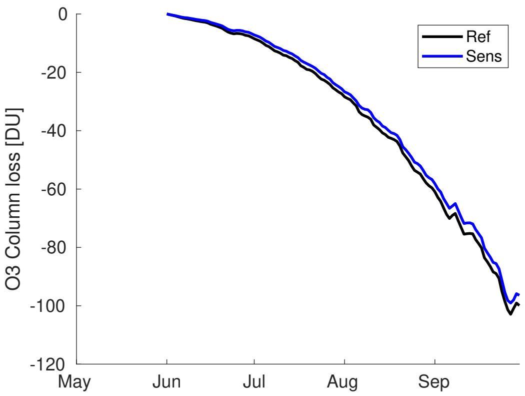

Figure 3. Vortex-averaged chemical loss of ozone modelled by ATLAS for the partial column from the lower model boundary at 157 hPa to 28.6 hPa. The black line shows the reference run initialized with MLS measurements from 2023, while the blue line shows the sensitivity run initialized with MLS water vapor data from 2022 (i.e., without the effect of Hunga Tonga on water vapor).

water vapor. For example, a change in water vapor from 5 ppm to 6 ppm increases the threshold temperature for ice by 1.1 K at 50 hPa (Marti & Mauersberger, 1993), and for NAT by 0.8 K (for a HNO_3 mixing ratio of 10 ppb) (D. Hanson & Mauersberger, 1988). STS has no defined threshold temperature for formation but shows a gradual increase of reaction rates and droplet volume with lower temperatures. However, an increase in water vapor from 5 ppm to 6 ppm has to a good approximation the same effect on the STS reactivity (time needed for the HCl+$ClONO_2$ reaction to completely deplete one of the reaction partners) as a temperature change of 1 K (D. R. Hanson & Ravishankara, 1994; Carslaw et al., 1995) (for 2 ppb HCl, 1 ppb $ClONO_2$, 0.15 ppb H_2SO_4, number density of droplets 10 cm^{-3}).
While these changes increase the volume inside the vortex where the formation of PSCs is possible, this can only have an effect before dehydration sets in. The effects of changes in threshold temperatures and STS reactivity are included in ATLAS. Figure 2 (b) shows that they have no large effect on ozone depletion.

- Changes in water vapor have an effect on the particle size distribution of all cloud types. There is more water vapor available above the saturation limit, and one might expect larger particle sizes and larger surface area densities. However, particle formation and growth is a complex process, and this might not be straightforward.
As in many chemistry and transport models, PSCs are treated in a somewhat simplified manner in ATLAS (Tritscher et al., 2021). For NAT and ice clouds, a constant number density is assumed, and a uniform particle size is then calculated from the HNO_3 and H_2O available above the saturation pressure. That is, the uniform particle size will simply increase in our model. For STS, a constant number density and a log-normal distribution is assumed that is scaled with the total liquid volume.
Figure 2 (b) shows that changes in size distribution have only a small effect on ozone depletion in ATLAS. However, particle growth and formation might be more complex in reality and the effect on ozone depletion may be larger. Changes in size distribution may also have an effect after dehydration sets in (i.e., differences in the size distribution of NAT, ice and STS PSCs caused by increased water vapor in May and June might be persistent or lead to changes in the size distribution in later months).

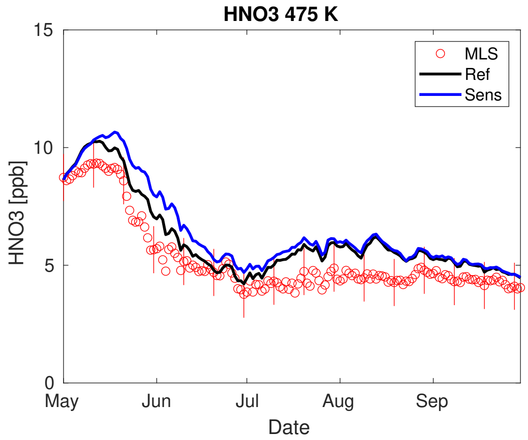

Figure 4. Vortex-averaged HNO_3 (gas phase) at 475 K potential temperature observed by MLS in 2023 (red dots) and modelled by ATLAS (blue and black lines). The black line shows the reference run initialized with MLS measurements from 2023, while the blue line shows the sensitivity run initialized with MLS water vapor data from 2022 (i.e., without the effect of Hunga Tonga on water vapor).

- Since larger particles have a greater fall velocity, dehydration might also be faster in 2023. However, this is not considered in the simple ATLAS dehydration parameterization. The good agreement between ATLAS and MLS suggests that dehydration might be a fast enough process so that the speed of the process does not matter for the amount of ozone depletion.
- Denitrification might also be affected by differences in the formation of the NAT particles. Denitrification is treated in a more sophisticated manner than dehydration in ATLAS and incorporates the nucleation, growth, sedimentation, and evaporation of individual particles with the DLAPSE model (Davies et al., 2005). Figure 4 shows that the changes in gas-phase HNO_3 (which are mainly caused by denitrification) are small between the reference run and the sensitivity run.

In summary, we have shown that while the Hunga Tonga-Hunga Ha'apai eruption increased water vapor in the emerging Southern Hemisphere stratospheric polar vortex by 20–40 % in 2023, ozone values at the end of September in the Antarctic ozone hole were in no way exceptional and were well within in the range of earlier years. ATLAS model runs indicate that the direct effect of the increased water vapor on Antarctic ozone depletion was minor. The reason for this are the very low temperatures in the vortex, which limit water vapor to the saturation pressure and tend to reset any anomalies in water vapor through dehydration before they can have an effect on ozone loss. However, the ATLAS runs underestimate observed ozone loss in 2023 by about 30 % (in contrast to good agreement with observations in similar studies for other winters). Further studies would be needed to understand the causes of this discrepancy and whether it may be related to other effects from the Hunga Tonga-Huga Ha'apai eruption in addition to the increased water vapor and dehydration.

Open Research Section

ATLAS source code is available from the repository at https://gitlab.awi.de/iwohltmann/atlas-julia. MLS data are available at https://disc.gsfc.nasa.gov/datasets?page=1&keywords=AURA%20MLS. ECMWF ERA5 data are available at Hersbach et al. (2017), doi:10.24381/cds.143582cf.

Acknowledgments

ECMWF ERA5 and ERA5T data (Hersbach et al., 2017) was downloaded from the Copernicus Climate Change Service (C3S) (2023). The results contain modified Copernicus Climate Change Service information 2023. Neither the European Commission nor ECMWF is responsible for any use that may be made of the Copernicus information or data it contains.

Work at the Jet Propulsion Laboratory, California Institute of Technology, was carried out under a contract with the National Aeronautics and Space Administration (80NM0018D0004). G. L. Manney was supported by the Jet Propulsion Laboratory (JPL) Microwave Limb Sounder team under JPL subcontract #1521127 to NWRA.

We thank Peter von der Gathen for helpful comments and discussion.

References

Carr, J. L., Horváth, Á., Wu, D. L., & Friberg, M. D. (2022). Stereo plume height and motion retrievals for the record-setting Hunga Tonga-Hunga Ha'apai eruption of 15 January 2022. *Geophys. Res. Lett.*, *49*. doi: 10.1029/2022GL098131

Carslaw, K. S., Clegg, S. L., & Brimblecombe, P. (1995). A thermodynamic model of the system HCl-HNO3-H2SO4-H2O, including solubilities of HBr, from < 200 to 328 k. *J. Phys. Chem.*, *99*(29), 11557-11574. doi: 10.1021/j100029a039

Davies, S., Mann, G. W., Carslaw, K. S., Chipperfield, M. P., Kettleborough, J. A., Santee, M. L., … Sugita, T. (2005). 3-D microphysical model studies of Arctic denitrification: comparison with observations. *Atmos. Chem. Phys.*, *5*, 3093-3109. doi: 10.5194/acp-5-3093-2005

Hanson, D., & Mauersberger, K. (1988). Laboratory studies of the nitric acid trihydrate: Implications for the south polar stratosphere. *Geophys. Res. Lett.*, *15*(8), 855-858. doi: 10.1029/GL015i008p00855

Hanson, D. R., & Ravishankara, A. R. (1994). Reactive uptake of ClONO2 onto sulfuric acid due to reaction with HCl and H2O. *J. Phys. Chem.*, *98*(22), 5728-5735. doi: 10.1021/j100073a026

Hersbach, H., Bell, B., Berrisford, P., S., Hirahara, Horányi, A., Muñoz-Sabater, J., … Thépaut, J.-N. (2017). Complete ERA5 from 1940: Fifth generation of ECMWF atmospheric reanalyses of the global climate. Copernicus Climate Change Service (C3S) Data Store (CDS). (Accessed on DD-MMM-YYYY). doi: 10.24381/cds.143582cf

Hersbach, H., Bell, B., Berrisford, P., Hirahara, S., Horányi, A., Muñoz-Sabater, J., … Thépaut, J.-N. (2020). The ERA5 global reanalysis. *Quarterly Journal of the Royal Meteorological Society*, *146*, 1999-2049. doi: 10.1002/qj.3803

Lait, L. R. (1994). An alternative form for potential vorticity. *J. Atmos. Sci.*, *51*(12), 1754-1759.

Livesey, N. J., Read, W. G., Wagner, P. A., Froidevaux, L., Santee, M. L., Schwartz, M. J., … Lay, R. R. (2022). *Earth Observing System (EOS) Aura Microwave Limb Sounder (MLS) version 5.0x level 2 and 3 data quality and description document.* JPL D-105336 Rev. B.

Manney, G. L., Santee, M. L., Lambert, A., Millán, L. F., Minschwaner, K., Werner, F., … Wang, T. (2023). Siege in the southern stratosphere: Hunga Tonga-Hunga Ha'apai water vapor excluded from the 2022 Antarctic polar vortex. *Geophys. Res. Lett.*, *50*. doi: 10.1029/2023GL103855

Marti, J., & Mauersberger, K. (1993). A survey and new measurements of ice vapor pressure at temperatures between 170 and 250 k. *Geophys. Res. Lett.*, *20*, 363-366. doi: 10.1029/93GL00105

Millán, L., Santee, M. L., Lambert, A., Livesey, N. J., Werner, F., Schwartz, M. J.,

… Froidevaux, L. (2022). The Hunga Tonga-Hunga Ha'apai hydration of the stratosphere. *Geophys. Res. Lett.*, *49*. doi: 10.1029/2022GL099381

Proud, S. R., Prata, A. T., & Schmauß, S. (2022). The January 2022 eruption of Hunga Tonga-Hunga Ha'apai volcano reached the mesosphere. *Science*, *378*(6619), 554-557. doi: 10.1126/science.abo407

Schoeberl, M. R., Wang, Y., Ueyama, R., Taha, G., Jensen, E., & Yu, W. (2022). Analysis and impact of the Hunga Tonga-Hunga Ha'apai stratospheric water vapor plume. *Geophys. Res. Lett.*. doi: 10.1029/2022GL100248

Tritscher, I., Pitts, M. C., Poole, L. R., Alexander, S. P., Cairo, F., Chipperfield, M. P., … Peter, T. (2021). Polar stratospheric clouds: Satellite observations, processes, and role in ozone depletion. *Reviews of Geophysics*, *59*(2). doi: 10.1029/2020RG000702

Vömel, H., Evan, S., & Tully, M. (2022). Water vapor injection into the stratosphere by Hunga Tonga-Hunga Ha'apai. *Science*, *377*, 1444-1447. doi: 10.1126/science.abq2299

Wohltmann, I., Lehmann, R., & Rex, M. (2010). The Lagrangian chemistry and transport model ATLAS: simulation and validation of stratospheric chemistry and ozone loss in the winter 1999/2000. *Geosci. Model Dev.*, *3*, 585-601.

Wohltmann, I., & Rex, M. (2009). The Lagrangian chemistry and transport model ATLAS: validation of advective transport and mixing. *Geosci. Model Dev.*, *2*, 153-173.

Wohltmann, I., von der Gathen, P., Lehmann, R., Deckelmann, H., Manney, G. L., Davies, J., … Rex, M. (2021). Chemical evolution of the exceptional Arctic stratospheric winter 2019/2020 compared to previous Arctic and Antarctic winters. *J. Geophys. Res. Atmos.*, *126*. doi: 10.1029/2020JD034356